



NLR-TP-2004-320

Acoustic array measurements of a 1:10.6 scaled Airbus A340 model

S. Oerlemans and P. Sijtsma

This report is based on AIAA paper 2004-2924 presented at the 10th AIAA/CEAS Aeroacoustics Conference in Manchester, UK on 10-12 May 2004.

This report may be cited on condition that full credit is given to NLR and the authors.

Customer: National Aerospace Laboratory NLR
Working Plan number: AV.1.C.1
Owner: National Aerospace Laboratory NLR
Division: Aerospace Vehicles
Distribution: Unlimited
Classification title: Unclassified
August 2004

Approved by author: SO 19/8/04	Approved by project manager: fS 19/8/04	Approved by project managing department: Gen 23/8/04
---------------------------------------	--	---



Contents

I. Introduction	3
II. Open Jet Test	5
III. Closed Test Section	6
IV. Conclusions	8
References	8

19 Figures

(16 pages in total)



Acoustic Array Measurements of a 1:10.6 Scaled Airbus A340 Model

Stefan Oerlemans* and Pieter Sijtsma*

National Aerospace Laboratory NLR, Emmeloord, The Netherlands

Acoustic array measurements were carried out on a 1:10.6 scaled Airbus A340 model. Tests were done in both the open jet and a closed test section of the DNW-LLF wind tunnel. The purpose of these measurements was to investigate several noise reduction concepts for high-lift devices (slats and flaps) in landing configuration. The possibilities and limitations of arrays for the determination of quantitative results are discussed. Besides the identification of dominant noise source regions with conventional beamforming, local source spectra were determined using a power integration method. For the open jet results, the integration method was applied with and without the 'diagonal removal' (DR) technique, in which the main diagonal of the cross-power matrix is discarded. It is shown that application of DR results in meaningful local spectra, whereas without DR the results are obscured by the influence of the main diagonal. On the other hand, by comparing integrated spectra with absolute sound levels on farfield microphones, it is shown that the application of DR, in combination with coherence loss, results in significantly reduced absolute levels. However, while the absolute sound levels can be too low, level differences between configurations can be accurately determined under certain conditions. From the closed test section array results, dominant source regions are identified as a function of frequency and angle-of-attack. These results are quantified by application of the integration method to several source areas on the wing. The local and overall effect of noise reduction devices is assessed. The effect of coherence loss on the absolute levels is investigated by varying the effective array size.

I. Introduction

AIRFRAME noise is one of the most important noise sources for a modern aircraft during approach. The dominant components of airframe noise are the landing gears and high lift devices (slats and flaps). Therefore, in the framework of the European SILENCE(R) project, a study was performed into airframe noise from the wings of an Airbus A340 aircraft during approach and landing. For this purpose, two test campaigns took place in the DNW-LLF wind tunnel, on a 1:10.6 scaled A340 model. The first wind tunnel test was carried out in the DNW open jet, with the purpose to optimize and validate several noise reduction concepts. A traversable farfield microphone boom was used in combination with an out-of-flow microphone array for the acoustic measurements. The second test campaign took place in a DNW closed test section, and intended to assess the aerodynamic properties of the most promising reduction devices. In parallel, acoustic wall array measurements were done to check the effectiveness of the (modified) noise reduction devices.

This paper deals with the acoustic array measurements that were done in both wind tunnel tests, and focuses on the quantification of array results. While location of noise sources with acoustic arrays is becoming a standard technique, the quantification of array results is still far from straightforward. For incoherent, separate monopole sources the absolute sound level corresponds to the peak level in the acoustic 'source plot'. However, in practice this situation seldom occurs. First, airframe noise sources are often distributed (e.g. slat noise, trailing edge noise). As a consequence, the peak level depends on the spatial extent of the source region and the resolution of the array (which again depends on frequency). The levels in the source plot also depend on the coherence between different regions of the distributed source. Second, the levels may be influenced by coherence loss. Coherence loss occurs when

* Research engineer, Aeroacoustics Department, P.O. Box 153, 8300 AD Emmeloord, The Netherlands.



sound is scattered by turbulence (e.g. in the shear layer of an open jet wind tunnel), and typically results in broader lobes with a lower peak level in the acoustic source plot. The effect increases with increasing frequency and increasing wind speed. Coherence loss also increases with increasing distance between array microphones. As a consequence, the outer microphones of an array often do not contribute to the reconstructed source signal at high frequencies. Since the reconstructed source signal (after delay & sum) is divided by the total number of microphones, this results in decreased source levels. The effects of coherence loss can be suppressed by using an integration contour rather than the peak level, to capture the broadening of the peak in the source plot. Also, by reducing the effective array size for higher frequencies, microphones that do not contribute to the reconstructed source signal are omitted.

A few years ago, Brooks *et al.*¹ presented a method for quantification of array results. They defined an integration area around the source region and calculated a frequency-dependent array calibration function, assuming a source distribution of uncorrelated monopoles. The method was applied to simulations of a line source and to measurements of a calibrator source and flap side-edge noise. It was found that absolute spectra of different sources could well be recovered from the phased array results, as long as the sources were not too close to the boundary of the integration box. Effects of coherence loss did not reduce the quality of the results significantly. However, when the array processing algorithm was applied after removal of the main diagonal from the cross-spectral density matrix, which is often done in situations with low signal-to-noise ratio, the integration technique was less reliable. This was probably caused by the fact that the cross-spectral density matrix is no longer positive-definite, which can lead to non-physical results in the source plot (negative 'source powers').

An integration method similar to Ref. 1 was used by Soderman *et al.*² to determine the relative importance of different source areas, but the reliability of the absolute levels was not investigated. Blacodon *et al.*³ also implemented an integration method and applied it to airframe noise from an aircraft model. Good agreement of overall integrated levels with single-microphone spectra was found. Although information on frequency range was not provided, the results may have been limited to relatively low frequencies, where coherence loss effects are small. Recently, the integration method was extended to moving sources by Sijtsma and Stoker⁴.

An alternative method for quantification of distributed sources (2D trailing edge noise) was presented in Ref. 5. Due to high tunnel background noise levels, Diagonal Removal (DR) was required and the integration method described above was not suitable. Therefore, peak levels at the trailing edge were translated to absolute source levels using an array calibration function, which was determined from simulations of an uncorrelated line source. It was shown that the assumption of an uncorrelated line source was justified and that the method yielded reliable absolute source levels. Coherence loss was shown not to be important for the relatively low frequencies presented. A similar method for quantification of trailing edge noise was applied in Ref. 6. Ref. 7 describes a method that uses an integration contour rather than peak levels, to suppress coherence loss effects at higher frequencies. A drawback of these methods is that they are only suitable for line sources.

For the present application, airframe noise sources on a 3D wing, a source quantification method was needed which can account for different types of noise sources. The method should also be applicable in closed wind tunnel test sections, where DR is mandatory due to high boundary layer pressure fluctuations at the microphones. Therefore, a modified version of the integration method¹ was implemented, which in case of DR discards negative source powers in both the simulated and measured source plots. When DR is not applied, the method is identical to the simplified method in Ref. 1. Prior to application in the DNW airframe noise tests, this method was applied to a number of test cases. When no DR was applied, the method provided accurate absolute noise levels for several cases (calibration source, helicopter model, train pantograph), even in the presence of coherence loss (Figure 1). However, when DR was applied, the method yielded too low levels when significant coherence loss was present (Figure 2). Surprisingly, in a closed test section the integration method provided accurate absolute levels at wind speeds up to 75 m/s, even though DR was applied (Figure 3). This suggests that coherence loss was not important in the closed test section.

The present paper describes the application of the integration method to the A340 wing noise measurements, and discusses the possibilities and limitations of acoustic arrays for the determination of quantitative results. Rather than presenting results for all configurations and conditions, only selected results will be shown to illustrate the characteristics of the array method. Section II deals with the open jet test, where the integration method is applied with and without DR. The results are analyzed and compared to the absolute sound level on a single microphone in the far field. In Section III the results for the closed test section are presented. The integration method (with DR) is applied to several source areas on the wing, and the local and overall effect of noise reduction devices is assessed. The effect of coherence loss on the absolute levels is investigated by varying the effective array size. The conclusions of this study are given in Section IV.



II. Open Jet Test

A. Test Set-Up

The tests were carried out in the DNW-LLF 8 x 6 m² open jet acoustic wind tunnel (Figure 4). The model was a 1:10.6 scaled Airbus A340 aircraft with a model span of about 6 m. The model had no landing gears, winglets or tail planes. The engines were simulated by through-flow nacelles. The model was mainly tested in landing configuration, but as a 'background noise' reference, measurements were also done in cruise ('clean') configuration. Due to the open jet set-up, the effective model angle of attack is smaller than the geometrical angle of attack. Here, the geometrical angles of attack will be mentioned. Measurements were done at wind speeds of 50, 60, and 70 m/s, and geometrical angles of attack of 3°, 7°, and 11°. The model was tested in baseline landing configuration and with several noise reduction devices on the wings.

Acoustic measurements were done with a farfield microphone boom below the right wing and an out-of-flow acoustic array below the left wing (Figure 4). Both the boom and the array could be traversed in flow direction, but here only array results for the position below the model will be shown. The distance between the array and the model was about 8 m. The array consisted of 120 ½-inch microphones (type LinearX M51) mounted in an open grid, and had a diameter of about 2.5 m. This relatively small array size was chosen to obtain good signal-to-noise-ratio even at high frequencies. The array microphones had wind screens to prevent wind-induced noise.

B. Data Acquisition and Processing

Acoustic data from the array microphones were synchronously measured at a sample frequency of 100 kHz and a measurement time of 60 s. A 500 Hz high-pass filter was used to enhance the dynamic range. The acoustic data were processed using a block size of 2048 with a Hanning window and an overlap of 50%, yielding almost 6000 averages and a narrowband frequency resolution of about 50 Hz. The frequency response of the individual array microphones was taken from calibration sheets.

Conventional beamforming⁸ was used to obtain acoustic source plots in 1/3-octave bands. To improve the resolution and further suppress background noise from the tunnel, the main diagonal in the cross power matrix (autopowers) could be discarded (Diagonal Removal). The effect of sound refraction by the tunnel shear layer was corrected using a simplified Amiet method⁹. The array scan plane was placed in the plane of the model and rotated in accordance with the angle of attack. The scan levels were normalized to a distance of 0.282 m $[(4\pi)^{-1/2}]$, so that for a monopole source the peak level in the source plot corresponds to the Sound Power Level.

The acoustic source plots were further processed to absolute source levels using an integration method similar to the 'simplified method' in Ref. 1. To prevent uncorrelated noise from obscuring the calculated airfoil noise levels, the main diagonal of the cross power matrix could be discarded. As explained in Section I, in this case negative source powers in both the simulated and measured source plots were discarded. Furthermore, a spatial window was applied to the microphone signals, which corrects for the variation in microphone density over the surface of the array, and which reduces the effective array aperture with increasing frequency. The purpose of this spatial shading was to improve the array resolution at low frequencies and to reduce coherence loss effects at high frequencies. The resulting acoustic spectra provide narrowband Sound Power Levels (in linear dB's) at model scale frequencies.

C. Discussion of Results

Typical examples of acoustic source plots, with and without diagonal removal, are shown in Figure 5. It can be seen that DR drastically improves the results, especially at higher frequencies. This indicates that the main diagonal of the crosspower matrix contains a lot of uncorrelated 'noise' which is not present in the off-diagonal terms. We will see below that these uncorrelated signals in the main diagonal do not originate from tunnel background noise, since 'background noise' levels (with the model in cruise configuration) are about 10 dB lower than the levels with the model in landing configuration. This suggests that the main diagonal contains airframe noise from the model, which has lost its phase relationship as a result of coherence loss, due to the propagation of the sound through the open jet shear layer.

To assess the ability of the power integration method to determine absolute noise levels, a rectangular integration contour was placed around both wings, and the resulting spectra were compared to the corresponding single-microphone spectra at the center of the array (Figure 6). As a 'background noise' reference, the single-microphone spectrum for the cruise configuration is also shown. Comparison of the single-microphone spectra confirms that the single-microphone spectrum for the landing configuration is due to airframe noise from the wings. It can be seen that without DR the power integration spectrum remains within a few dB of the single-microphone spectrum over the whole frequency range. With DR, the power integration spectrum underpredicts the absolute levels by up to



10 dB at high frequencies. This underprediction of absolute levels is probably due to the combination of DR with significant coherence loss, similar to the measurements on a calibration source prior to the airframe noise tests (Figure 2). Apparently this effect occurs despite the use of an integration contour rather than peak levels, and despite the use of a spatial window which reduces the effective array size with increasing frequency. Besides coherence loss, an additional reason for the low integrated levels with DR, may be the negative effect of a given source on the scan levels at adjacent source locations.

From the above observations it may be concluded that DR should not be applied to obtain accurate source levels. However, it will be shown in the following that this conclusion is not justified. As we have seen in Figure 5, the acoustic source plots without DR are dominated by uncorrelated (wing) noise in the main diagonal of the cross power matrix. This implies that the power integration results without DR are also dominated by this uncorrelated noise, which explains why the spectrum remains close to the single-microphone spectrum. It also means, however, that the very purpose of array measurements, obtaining *local* source information, is not possible without DR. This is illustrated in Figure 7 and Figure 8. Figure 7 shows the difference in noise from the left and the right wing, calculated using the power integration method with and without DR. Large differences are observed between the two 'delta spectra': whereas with DR large differences between the left and right wing are observed (up to more than 4 dB), the spectrum obtained without DR remains within 1 dB over the whole frequency range. If we look at the narrowband acoustic source plots for two closely spaced peak frequencies (Figure 8), it turns out that the large differences between the left and right wing are real. This illustrates that the power integration method with DR is able to determine local source characteristics, while without DR the results are completely obscured by uncorrelated noise in the main diagonal.

The above discussion shows that DR should be applied to obtain meaningful local spectra, but that the absolute levels are too low. Next, it is investigated whether level differences between configurations can be determined reliably. For this purpose, the power integration method (with DR) is applied to both wings, and the difference between two configurations (with and without slat track fairings) is compared to the difference in the single-microphone spectra (Figure 9). As can be seen, the differences agree quite well, and remain within 1 dB over the whole frequency range. This illustrates that, although the absolute levels are too low for both configurations, level *differences* can still be determined reliably. It should be noted that this may not hold when the amount of coherence loss is different for the two configurations, e.g. when the dominant source location changes from one configuration to the other. In this case the trajectory of sound from the source to the microphones differs, possibly resulting in different coherence loss effects and different absolute noise levels.

III. Closed Test Section

A. Test Set-Up

The tests were carried out in the DNW-LLF 8 x 6 m² closed test section (Figure 10). The model was the same as in the open jet tests. It had no landing gears and horizontal tail plane, but did have the vertical tail plane and winglets, in order to allow comparison to earlier aerodynamic measurements. The engines were simulated by through-flow nacelles. The model was mainly tested in landing configuration, but as a 'background noise' reference, measurements were also done in cruise ('clean') configuration. Measurements were done at wind speeds of 50, 60, and 70 m/s, and effective angles of attack of 3°, 7°, and 11°. The model was tested in the baseline landing configuration and with several noise reduction devices on the wings.

Acoustic measurements were done with a microphone array mounted in the tunnel floor below the right wing. During the acoustic measurements the model was placed 1.8 m above the array. The array consisted of 100 ½-inch microphones (type LinearX M51) flush-mounted in the floor plate, and had dimensions of about 0.5 x 0.6 m².

B. Data Acquisition and Processing

Data acquisition and processing were similar to the open jet test (Section II). Acoustic data from the array microphones were synchronously measured at a sample frequency of 120 kHz and a measurement time of 30 s. A 6 kHz high-pass filter was used to enhance the dynamic range. The acoustic data were processed using a block size of 2048 with a Hanning window and an overlap of 50%, yielding about 3500 averages and a narrowband frequency resolution of about 60 Hz. The frequency response of the individual array microphones was taken from calibration sheets.

The acoustic source plots were obtained using the same method as for the open jet measurements. Conventional beamforming was used and the main diagonal in the cross power matrix was discarded. The array scan plane was placed in the plane of the model and rotated in accordance with the angle of attack. The scan levels were again



normalized to a distance of 0.282 m $[(4\pi)^{-1/2}]$, so that for a monopole source the peak level in the source plot corresponds to the Sound Power Level. The acoustic source plots were further processed using the power integration method. The main diagonal of the cross power matrix was again discarded. No spatial window was applied to the microphone signals, since coherence loss effects were expected to be small (see Figure 3 and the next section). The resulting acoustic spectra provide narrowband Sound Power Levels (in linear dB's) at model scale frequencies.

C. Discussion of Results

Typical acoustic source plots are shown in Figure 11, as a function of model angle of attack. Note that for each source plot the color scale is automatically adjusted to the maximum level in the plot, so that the colors for different plots are not directly comparable. The dynamic range is always 12 dB. Some qualitative observations can be made from these plots: whereas for a low angle of attack the slats seem to be dominant, at higher angles of attack the outer engine and slat horn (at the junction of the slat and the fuselage) become more important. The importance of the slat horn increases with frequency. To quantify the dependence of the wing noise on angle of attack, the power integration method was applied to the wing. Since practically all noise sources were located at the leading edge of the wing, a leading edge integration region was chosen for efficiency reasons (Figure 12). Comparisons with a full wing integration region (Figure 12) only showed small differences: absolute levels generally agreed within 1.5 dB and relative levels (differences between configurations) within 0.5 dB.

Figure 13 shows the wing noise spectra (as obtained with the leading edge integration region) for the three angles of attack. As a 'background noise' reference the cruise configuration for the same wind speed is plotted as well. It can be seen that noise levels increase with increasing angle of attack, and that the differences are largest for higher frequencies. To further investigate the origin of these differences, several source areas were defined on the wing leading edge (Figure 14). By applying the power integration method to these source areas, a quantitative decomposition of the wing noise can be made (Figure 15). This plot confirms the qualitative observations from the source plots: for the low angle of attack the middle and outer wing are the dominant source regions for all frequencies, while at the highest angle of attack the outer engine (low frequencies) and slat horn (high frequencies) are dominant. This source decomposition as a function of frequency and angle of attack illustrates the strength of the integration method for obtaining local source information.

Besides the contributions of the separate source regions, Figure 15 also shows the sum of all leading edge regions. Such a summation can be tricky, since the different regions may overlap or one source may contribute to more than one integration region, which would result in an overestimation of the total source strength. However, when the overlap is small, and the integration regions are large enough with respect to the array resolution, the summation of different source regions should provide an accurate total source level. Indeed, when the sum of the leading edge sources was compared to the complete leading edge integration (Figure 12), the absolute levels were found to agree within 1.5 dB.

The power integration method can also be used to assess the effect of noise reduction concepts. Figure 16 shows the effect of a brush device at the slat horn. It can be seen that locally large reductions are obtained, while the noise sources at other locations maintain the same strength. To quantify the local and overall effect of this device, the integration method was applied to the slat horn region and to the complete leading edge integration region (Figure 17). This plot shows that while locally reductions up to 8 dB are obtained, the overall wing noise reduction is only 3 dB at most. This difference is due to the fact that the other noise sources on the wing are not reduced by the slat horn brush.

To assess the reliability of the absolute source levels obtained in the closed section, the effect of coherence loss was investigated. As we have seen for the open jet tests in Section II, the combination of DR with coherence loss leads to significantly reduced source levels. In the closed test section the effect is expected to be less important, since the array is smaller and the closed section boundary layer is thinner than the open jet shear layer (see also Figure 3). In the closed test section there is no absolute reference sound level to check this, since the levels at the array microphones are dominated by the tunnel wall boundary layer pressure fluctuations. However, there is an alternative method to estimate the importance of coherence loss in the closed test section. The coherence between the signals on two microphones decreases with increasing distance between the microphones. Thus, *if* coherence loss is important, re-processing the measurements with a reduced array size should result in increased integrated array levels. Therefore, the two outer 'rings' of the microphone array were successively removed in the processing (Figure 18) and the integrated spectra were compared to the spectrum obtained with the full array (Figure 19). It can be seen that only a slight increase in spectral levels occurs when the array size is decreased (less than 1 dB up to 25 kHz model scale). This shows that the effect of coherence loss is quite small. It should be noted that, even when coherence loss is not important, the negative effect of a given source on the scan levels at adjacent source locations (when DR is applied) may also lead to reduced absolute levels⁴.



IV. Conclusions

Acoustic array measurements were carried out on a 1:10.6 scaled Airbus A340 model. Tests were done in both the open jet and a closed test section of the DNW-LLF wind tunnel. Besides the identification of dominant noise source regions with conventional beamforming, local source spectra were determined using a power integration method. For the open jet results, it was shown that application of Diagonal Removal (DR) results in meaningful local spectra, whereas without DR the results are obscured by the influence of the main diagonal. On the other hand, by comparing integrated spectra with absolute sound levels on farfield microphones, it was shown that the application of DR, in combination with coherence loss, results in significantly reduced absolute levels. However, while the absolute sound levels can be too low, level differences between configurations can be accurately determined under certain conditions. From the closed test section array results, dominant source regions were identified as a function of frequency and angle-of-attack. These results were quantified by application of the integration method (with DR) to several source areas on the wing. The integration method also enabled to distinguish between the local and overall effect of noise reduction devices. The effect of coherence loss in the closed test section was shown to be small by varying the effective array size.

References

- ¹ Brooks, T.F., and Humphreys, W.M., "Effect of directional array size on the measurement of airframe noise components", AIAA paper 99-1958, 1999.
- ² Soderman, P.T. *et al.*, "Airframe Noise Study of a CRJ-700 Aircraft Model in the NASA Ames 7- by 10-foot Wind Tunnel No. 1", AIAA paper 2002-2406, 2002.
- ³ Blacodon, D., and Elias, G., "Level estimation of extended acoustic sources using an array of microphones", AIAA paper 2003-3199, 2003.
- ⁴ Sijtsma, P., and Stoker, R.W., "Determination of Absolute Contributions of Aircraft Noise Components using Fly-Over Array Measurements", AIAA paper 2004-2958, 2004.
- ⁵ Oerlemans, S., and Sijtsma, P., "Determination of Absolute Levels from Phased Array Measurements Using Spatial Source Coherence", AIAA paper 2002-2464, 2002.
- ⁶ Hutcheson, F.V., and Brooks, T.F., "Effects of Angle of Attack and Velocity on Trailing Edge Noise", AIAA paper 2004-1031, 2004.
- ⁷ Oerlemans, S., and Migliore, P., "Aeroacoustic Wind Tunnel Tests of Wind Turbine Airfoils", AIAA paper 2004-3042, 2004.
- ⁸ Johnson, D.H., and Dudgeon, D.E., "Array Signal Processing", Prentice Hall, 1993.
- ⁹ Amiet, R.K., "Refraction of Sound by a Shear Layer", Journal of Sound and Vibration, Vol. 58, No. 2, pp. 467-482, 1978.



Figures

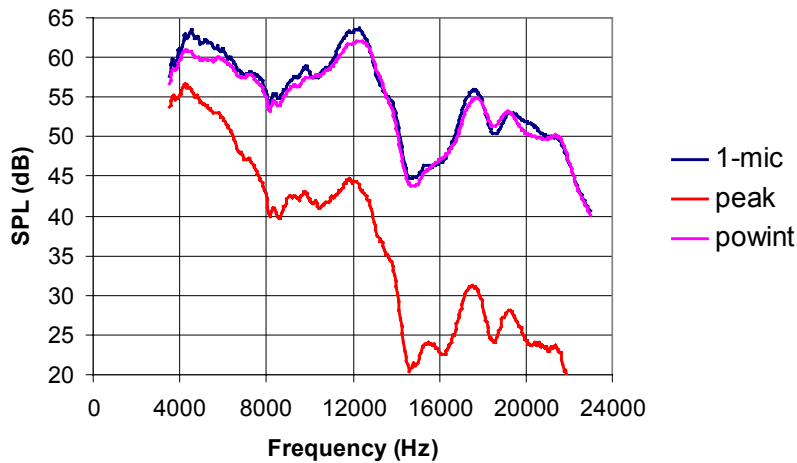


Figure 1: Validation of the power integration method (without Diagonal Removal) using a calibration source in the DNW-LLF open jet, at a wind speed of 50 m/s. While the peak levels in the acoustic source plot are much too low due to coherence loss, the integrated levels show good agreement with the single-microphone level.

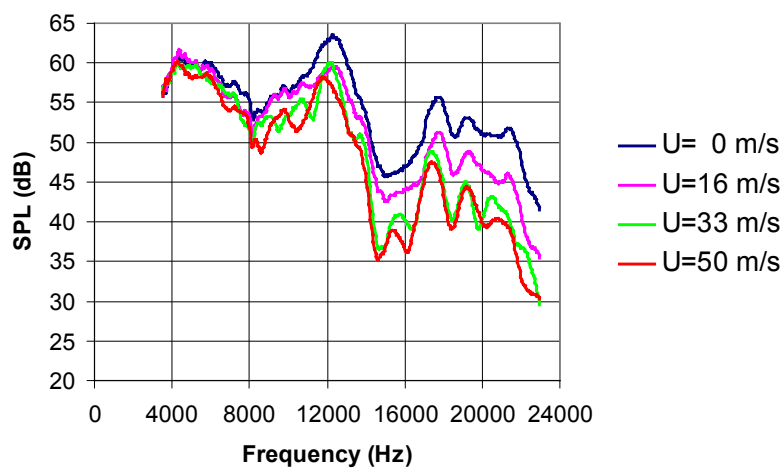


Figure 2: Application of the power integration method (with Diagonal Removal) to a calibration source in the DNW-LLF open jet, at several wind speeds. The combination of Diagonal Removal with coherence loss leads to significantly reduced integrated levels at higher wind speeds.

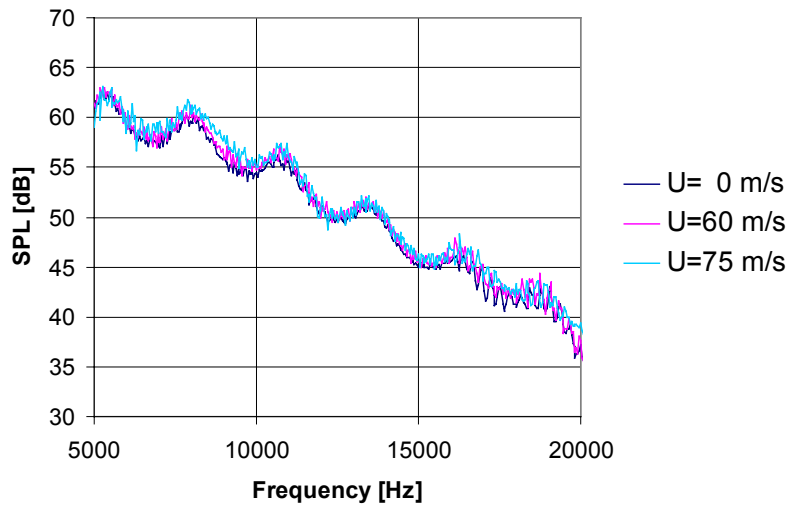


Figure 3: Application of the power integration method (with Diagonal Removal) to a calibration source in the DNW-LST closed test section. The good agreement between the integrated levels at the different wind speeds suggests that coherence loss is not important.

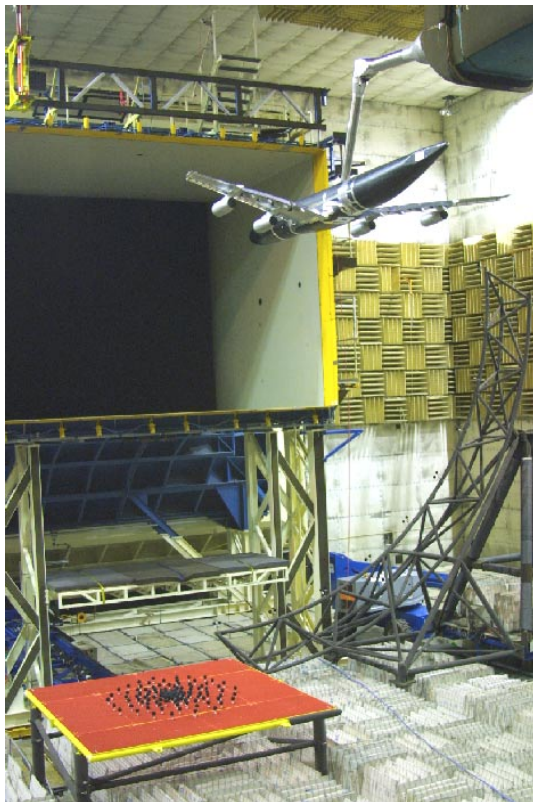


Figure 4: Test set-up in DNW open jet. The out-of-flow microphone array is shown in red.

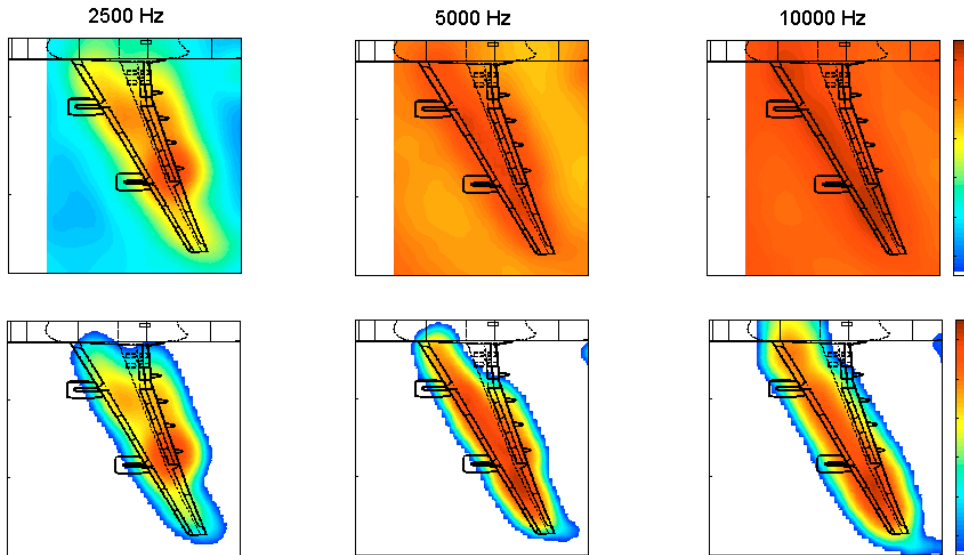


Figure 5: Typical acoustic source plots without (upper row) and with (lower row) Diagonal Removal. The dynamic range of the color scale is 12 dB.

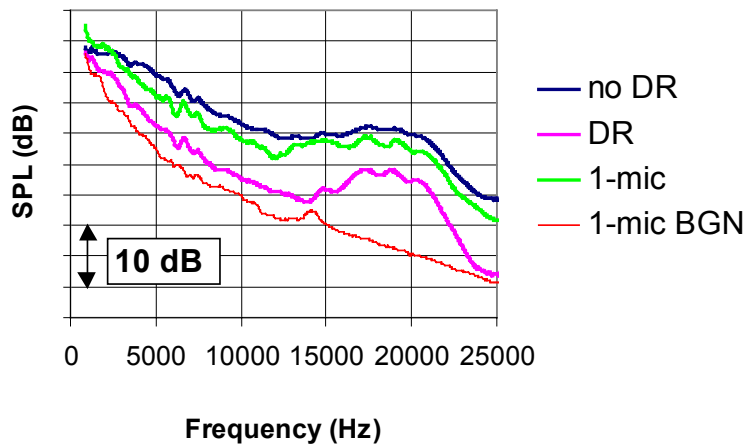


Figure 6: Comparison of integrated wing noise spectra for the model in landing configuration (with and without Diagonal Removal) to single-microphone spectrum. The single-microphone spectrum for the cruise configuration is shown as a 'background noise' (BGN) reference.

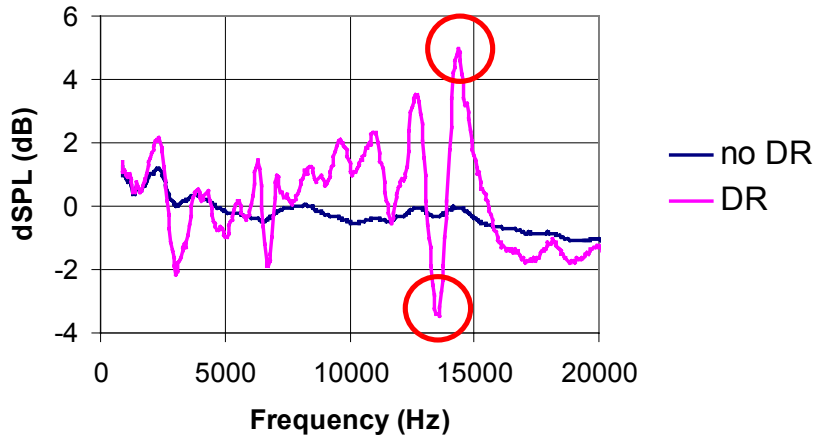


Figure 7: Difference in noise from left and right wing, calculated using integration method with and without Diagonal Removal. The source plots corresponding to the peaks at 13.6 and 14.4 kHz are shown in Figure 8.

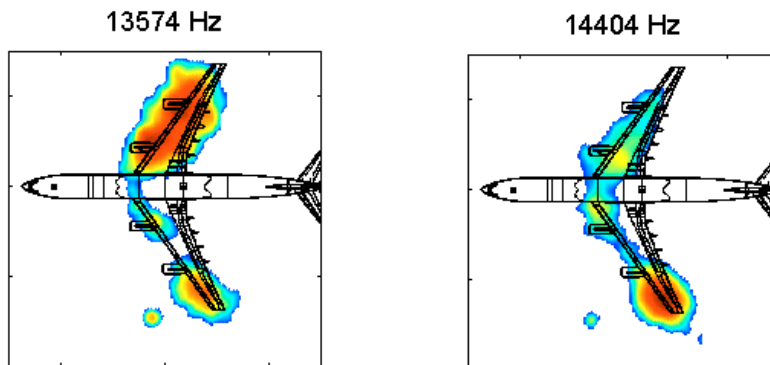


Figure 8: Narrowband acoustic source plots (with Diagonal Removal), corresponding to the integrated spectra in Figure 7.

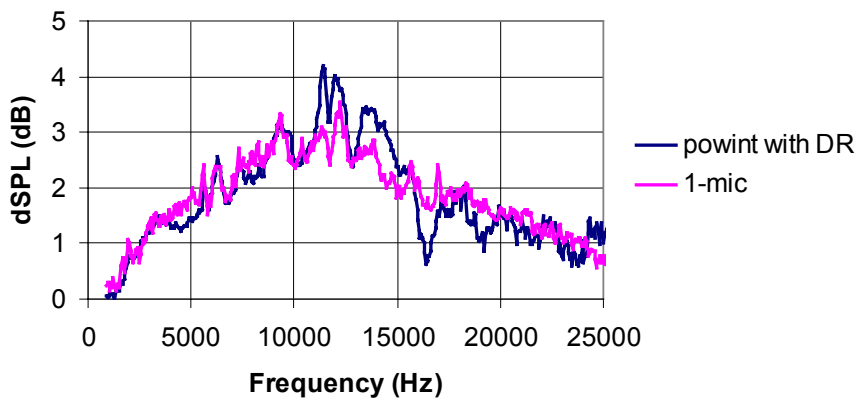


Figure 9: Difference in wing noise between two configurations (effect of slat track fairings), calculated from power integration method (with DR) and from single-microphone spectra.

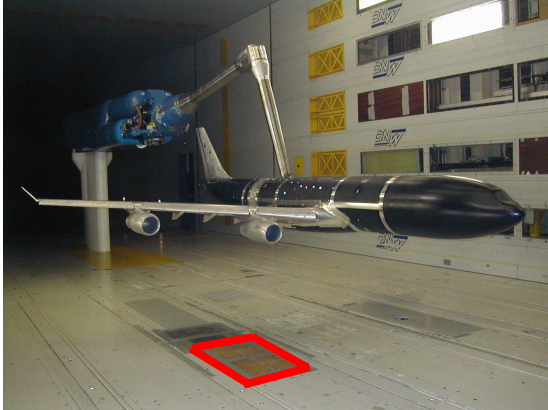


Figure 10: Test set-up in DNW closed section. The position of the wall array is indicated in red.

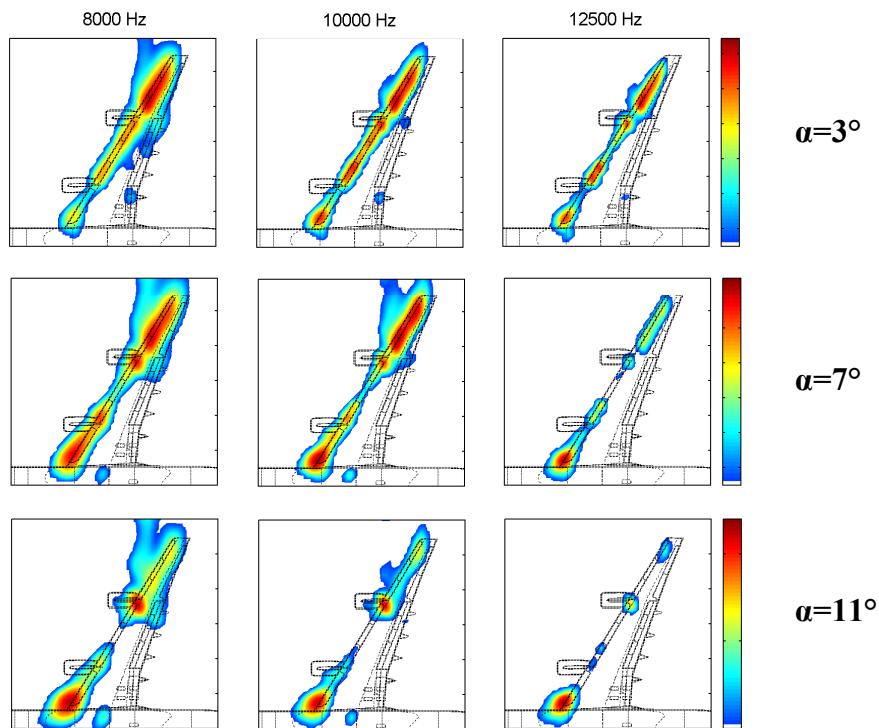


Figure 11: Effect of angle-of-attack on the source characteristics of the aircraft model in landing configuration, at a wind speed of 70 m/s. The dynamic range of the color scale is 12 dB.

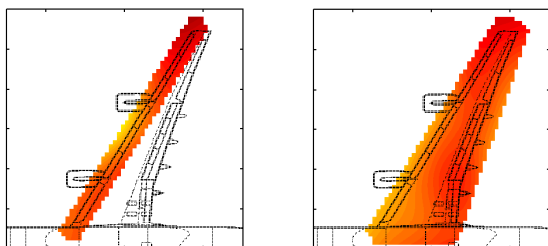


Figure 12: Power integration regions for leading edge and full wing.

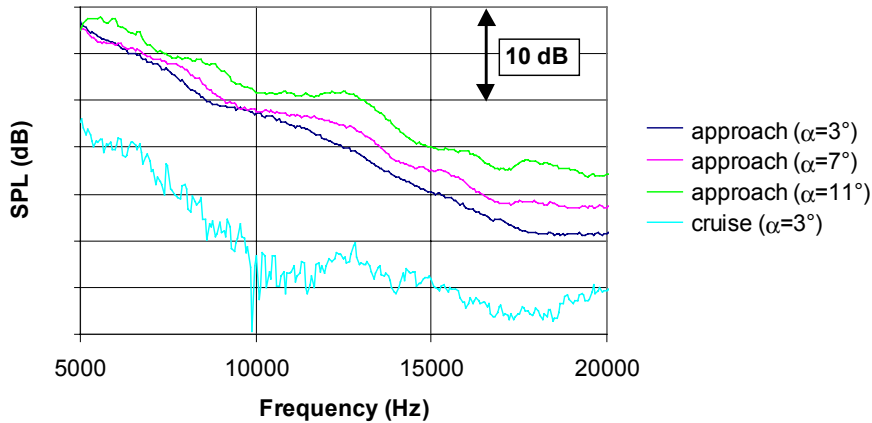


Figure 13: Effect of angle-of-attack on wing noise in landing configuration, at a wind speed of 70 m/s. The cruise configuration is shown as a 'background noise' reference.

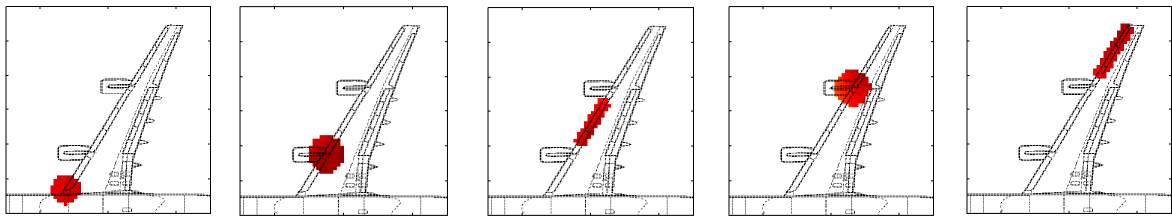


Figure 14: Leading edge regions used for local source quantification. From left to right: slat horn, inner engine, middle wing, outer engine, outer wing.

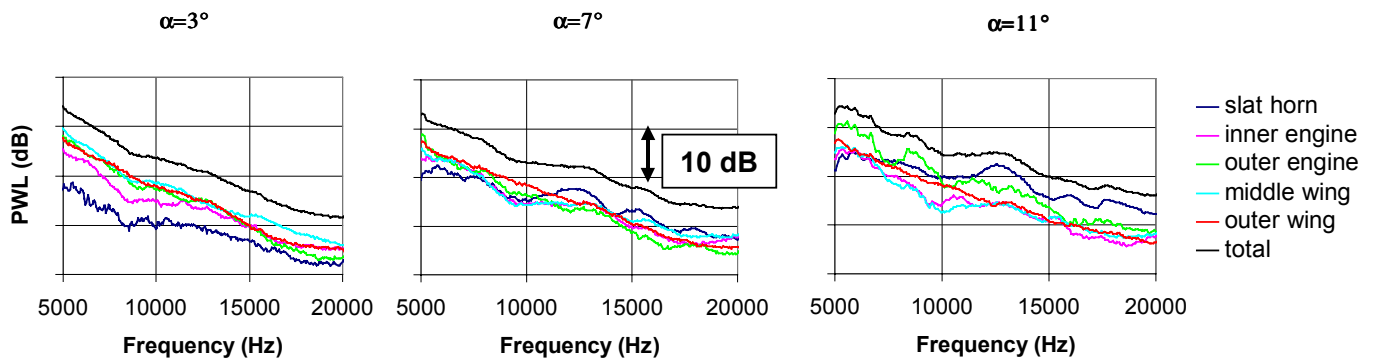


Figure 15: Decomposition of wing noise sources as a function of angle of attack.

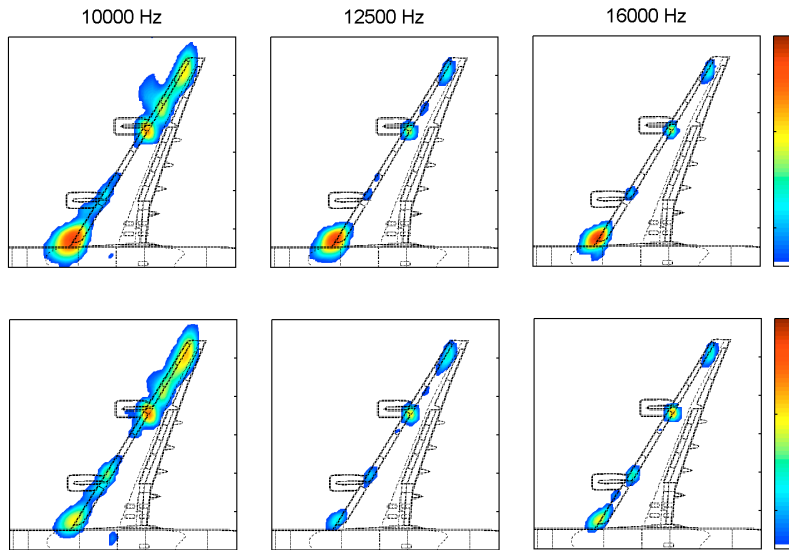


Figure 16: Acoustic source plots for the landing configuration at 60 m/s and $\alpha=11^\circ$, without (upper row) and with (lower row) brush device at the slat horn. The color scales are the same for the upper and lower row.

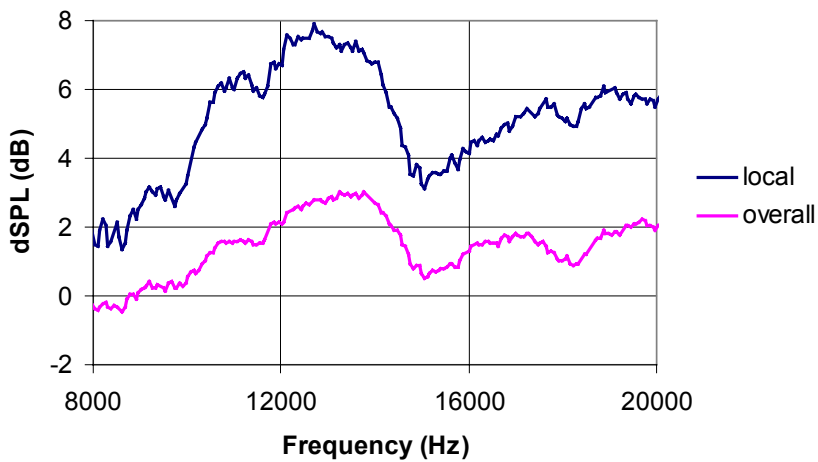


Figure 17: Local and overall noise reduction from brush device at slat horn. For the local effect the slat horn integration region was used, for the overall effect the complete leading edge integration region.

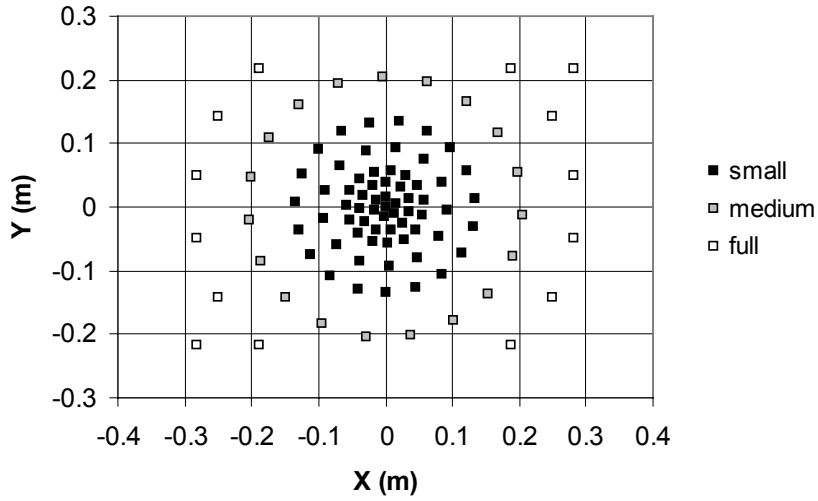


Figure 18: Different array sizes used for processing.

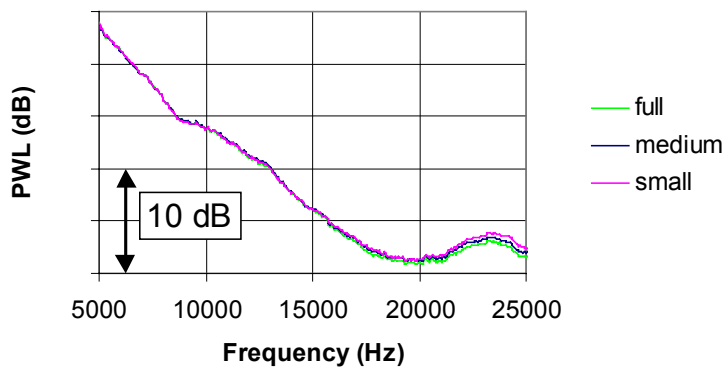


Figure 19: Effect of array size on integrated wing noise levels.